SAND--89-0633C

DE89 008580

MATERIALS ANALYSIS WITH NUCLEAR MICROPROBES: SUPERCONDUCTORS AND BURIED CONDUCTORS

J. C. Barbour and B. L. Doyle[1]

Nuclear microprobe analysis (NMA) is a unique form of microbeam analysis in that it combines high lateral resolution with the high depth resolution techniques of conventional ion beam analysis (IBA) to nondestructively determine sample composition in three dimensions. By using depth sensitive IBA techniques (e.g., Rutherford Backscattering Spectrometry (RBS), Enhanced Backscattering Spectrometry (EBS) or Elastic Recoil Detection (ERD)), NMA finds its greatest utility in analyses requiring the following information: 1) 1-100 ppm sensitivity, 2) nondestructive three-dimensional depth profiling, and 3) quantitative light element analysis (e.g., the first two rows of the periodic table). This paper demonstrates the continuing evolution of NMA capabilities through two examples. First, the unique capabilities afforded NMA are shown in a simple yet accurate method to measure both oxygen and metal atom concentrations in Y-Ba-Cu-O alloys with micro-area ion beam analysis. Second, a NMA of buried tungsten lines in a silicon wafer demonstrates the complementary nature of information determined by NMA and scanning electron microscopy (SEM).

SANDIA NUCLEAR MICROPROBE

The Sandia nuclear microprobe[1,2] is one of 5 beam lines attached to an EN tandem Van de Graaff accelerator. This accelerator is used to obtain high energy ion beams which are focussed onto object slits set at 25x3 μm -- horizontal x vertical. The beam is then defined by an aperture slit (1

1Sandia National Laboratories, Albuquerque, NM 87185. The work was supported by the U.S. Department of Energy under contract DE-AC04-76DP00789. The authors thank J.A. Knapp, N.D. Wing, T.L. Aselage, and R.S. Blewer for their assistance in this work.

MASTER

DISTRIBUTION OF THIS DOCUMENT IS UNLIMITED

DISCLAIMER

This report was prepared as an account of work sponsored by an agency of the United States Government. Neither the United States Government nor any agency thereof, nor any of their employees, makes any warranty, express or implied, or assumes any legal liability or responsibility for the accuracy, completeness, or usefulness of any information, apparatus, product, or process disclosed, or represents that its use would not infringe privately owned rights. Reference herein to any specific commercial product, process, or service by trade name, trademark, manufacturer, or otherwise does not necessarily constitute or imply its endorsement, recommendation, or favoring by the United States Government or any agency thereof. The views and opinions of authors expressed herein do not necessarily state or reflect those of the United States Government or any agency thereof.

DISCLAIMER

Portions of this document may be illegible in electronic image products. Images are produced from the best available original document.

mm x 1 mm) which is upstream from a small magnetic hexapole lens. A magnetic quadrupole doublet lens, which can steer the beam electrostatically as well as focus it magnetically, is positioned immediately after the hexapole lens. This quadrupole doublet lens is used for final focussing of the beam onto the target. The target chamber is kept at high vacuum ($<10^{-6}$ Torr) and contains a secondary electron detector which is used for imaging the sample surface, an annular particle detector which is used for RBS and EBS, and a Si(Li) detector which is used for particle induced x-ray emission (PIXE, when using proton beams; or HIXE, when using He beams). The distance between the doublet lens and the target can be as small as 5 cm, which results in a horizontal demagnification of 1/25 and a vertical demagnification of 1/3. These optics should define a 1 μm diameter spot on target, and typically a 1-2 μm diameter spot is obtained. The operational portion of the nuclear microprobe, from the object slits to the target chamber, is 1.5 m long.

The focussing procedure for the nuclear microprobe has previously[3] been described in detail, and therefore only a brief description will be given here. The object and aperture slits are opened to allow a broad beam to illuminate the hexapole and quadrupole lenses, and the beam is imaged on a fluorescing glass slide in the target chamber. The initial image (100-300 μm on a side) is an 8-pointed star defined by the 8 pole pieces of the doublet lens. Aberrations in the lens system are removed by adjusting the quadrupole lens to form a symmetric star pattern such that the principal focal planes of two singlets are exactly 90 degrees apart. The aperture slits are inserted to define a smaller spot from just the center portion of the beam and the quadrupole is used to focus the beam to a spot $\approx$ 50 μm on a side. At this point, aberrations from the quadrupole

lens, which may cause the spot to appear as a trapezoid, are removed by adjusting the hexapole lens to obtain a rectangular spot. The quadrupole lens can then be readjusted for optimum focus. The object slits are partially closed until the image (at optimum focus) becomes a dim circular spot. (An iterative adjustment of the quadrupole and hexapole lenses are usually required during this step.) A computer controlled scanning system is used to raster the beam over a 400 mesh (25 μm wide holes) Cu TEM grid and the secondary electron image of this grid is observed on an oscilloscope. The final focus is obtained by adjusting the quadrupole and the object slits to optimize the clarity of the secondary electron image.

Computer assisted data collection and reduction are essential for NMA in order to process the vast amount of information gathered, and because of the complexity of some of the techniques. A typical data acquisition system collects data in the following forms: yield (counts from an SCA) vs X and Y position -- useful for imaging secondary electrons and useful for producing single element maps with RBS, NRA or PIXE; yield vs event energy (E) and position -- useful for line scans; and yield vs E, X and Y -- useful for mapping multiple elements with PIXE and NRA, or for three-dimensional profiling with RBS, ERD or EBS.

SUPERCONDUCTORS

The dependence of superconductivity on the oxygen content in high temperature superconducting (HTSC) alloys has stimulated new studies to measure oxygen concentrations from grain-to-grain in polycrystalline materials. The orthorhombic $YBa_2Cu_3O_{7-\delta}$ phase (1237 composition) has been identified[4] as the superconducting phase with properties that are sensitive to the oxygen content; and weight loss measurements[5] have been used to determine the level of oxygen in homogeneous bulk samples (demonstrating a

loss of superconductivity for $\delta > 0.5$). Further, SEM analyses in conjunction with energy dispersive x-ray spectroscopy have been used to measure metal atom concentrations with high lateral resolution[6], but these SEM-based techniques do not yield information on oxygen. Therefore, we have used EBS, HIXE and RBS in the nuclear microprobe to measure the uniformity of the oxygen and metal atom concentrations of a bulk Y-Ba-Cu-O alloy.

Laterally nonuniform bulk samples were prepared by cooling a melt containing Y_2O_3, BaO and CuO. The melt was cooled in an oxygen ambient and analyzed, as-cooled, without an annealing treatment to form a homogeneous superconductor. A mixture of phases was observed at a magnification of 100X in an optical microscope. The sample was determined to be non-superconducting, but the presence of several phases suggested that small grains of 1237 material may be isolated within a matrix of non-superconducting alloy. A portion of the sample which was near the edge of the melt was analyzed by NMA to determine if regions of material with the proper 1237 composition were present. A 2 μm diameter He beam, at an energy of 8.7 MeV (scattering angle of 167°), was used to analyze several areas of the sample; and in each area, the beam was rastered over a region 100μmx100μm. Figure 1 is representative of the backscattering and HIXE results from this sample. The HIXE maps (at right) show that the Y-rich regions (dark in the upper map) correspond to Ba-poor regions (light in the lower map). In comparison, the Cu x-ray signal and secondary electron image showed little contrast over the same area. These HIXE maps also show that the Y-rich grains range in size from 10 μm to 30 μm in diameter and are embedded in a Ba-rich matrix. Based on these elemental maps, the beam was positioned at a point and RBS spectra (shown at left) were collected in

each region in order to quantitatively determine the composition of the matrix and the embedded grains.

Ion backscattering analysis has been described by Chu et al.[7] for the case in which the ion scattering cross section (σ) obeys the Rutherford cross-section formula (σ) to within a few percent. At 8.7 MeV, α scattering from Ba is Rutherford, but the oxygen scattering cross section is non-Rutherford. The yield for Rutherford scattering is greater for high Z elements (e.g., Ba) than for low Z elements (e.g., O), and the amount of backscattering decreases as the incident ion energy increases. Therefore, low energy ($\leq$3.5 MeV α) RBS of superconductors is more accurate for measuring the heavy element concentrations than for measuring the oxygen content because the small O signal (low σ for oxygen) sits on the large metal atom background. However, high energy ion beams take advantage of the fact that the scattering cross sections for the heavy elements decrease as σ decreases, thereby yielding a lower background and better counting statistics for oxygen (greater accuracy). Reference 8 examined the use of EBS with a broad beam of 8.7 MeV He and determined that σ(oxygen) is 22 times greater than σ; and therefore the oxygen content in a thin film HTSC could be determined to within 2-3%.

The EBS technique given above was used in the present experiment to measure the oxygen content of the bulk sample with the 2 μm lateral resolution afforded NMA. The oxygen cross section was found to be enhanced over σ(oxygen) by a factor of 27 for the scattering geometry in this experiment. The following table summarizes the capabilities of EBS in the nuclear microprobe:

DISCLAIMER

This report was prepared as an account of work sponsored by an agency of the United States Government. Neither the United States Government nor any agency thereof, nor any of their employees, makes any warranty, express or implied, or assumes any legal liability or responsibility for the accuracy, completeness, or usefulness of any information, apparatus, product, or process disclosed, or represents that its use would not infringe privately owned rights. Reference herein to any specific commercial product, process, or service by trade name, trademark, manufacturer, or otherwise does not necessarily constitute or imply its endorsement, recommendation, or favoring by the United States Government or any agency thereof. The views and opinions of authors expressed herein do not necessarily state or reflect those of the United States Government or any agency thereof.

EBS of ^{16}O with 8.7 MeV α in the Nuclear Microprobe

θ	σ/σ	Analysis Range	Depth Resolution	Lateral Resolution	Sensitivity
167°	27	1.7 μm	50 nm	2 μm	10^{21} /cm^3

where theta is the backscattering angle and σ/σ is the cross-section ratio relative to Rutherford scattering. The analysis range is limited to a few microns because σ(oxygen) oscillates strongly with energy below 8.3 MeV, as reflected in the RBS spectra below 2.5 MeV. The shaded portions of the oxygen signals in figure 1 correspond to a depth of $\approx$ 1.7 μm in $YBa_2Cu_3O_7$. The depth resolution is determined from the energy resolution of the particle detector and the stopping power of α particles in an Y-Ba-Cu-O alloy. The accuracy of EBS given above is also applicable for NMA and yields a detectable variation in δ of $\Delta\delta$=0.3 (where 7-δ is the subscript for the 1237 composition).

Surface scattering energies for the constituent atoms in the RBS spectra of figure 1 are: E= 7.754 MeV, E= 7.282 MeV, E= 6.782 MeV, E= 3.170 MeV. The signal from the Y, Cu, and O atoms appear at lower energies in the RBS spectra than the Ba signal, and overlap the Ba signal because the sample is a bulk alloy. However, the Y and Ba signals are sufficiently separated such that the oxygen yield can be measured relative to the Ba yield, alone. The equations from conventional backscattering spectrometry[7] can then be applied to determine the oxygen content using σ/σ = 27, for oxygen. The concentration scales plotted next to the yield for each element are given in atoms per formula unit.

Results of NMA showed that the matrix and grains were uniform in composition in all three dimensions. The Ba-rich matrix had a composition of $YBa_2Cu_3O_6$, which is the composition for the non-superconducting

tetragonal phase; and the Y-rich grains had a composition of Y_2BaCuO_5, which is the composition for a semiconducting phase. Therefore, these results confirmed the absence of a superconducting phase in the as-cooled sample and showed that a post-melt oxygen anneal is necessary for superconductor formation. A NMA measurement of the matrix oxygen content proved critical to this evaluation.

BURIED TUNGSTEN CONDUCTIVE LAYERS

Buried conductors in single crystal Si wafers are of interest for metallization of three-dimensional device structures. Multilevel metallization may increase both device speed and radiation hardness. This work investigates a process in which a W layer was buried beneath a Si island through the use of low pressure chemical vapor deposition (LPCVD).[9] The W is selectively deposited in a porous Si layer beneath the island leaving the single crystal island in an undamaged state which is compatible with further processing to form microcircuits. The object of this work is to characterize a patterned Si wafer exposed to the tungsten LPCVD treatment, and in particular to characterize the extent of W deposition and reaction around the Si island. The samples were patterned in long strips of Si islands $\approx$ 40 μm wide and 9 μm apart. Nuclear microprobe analysis and scanning electron microscopy were used to determine the extent of the W deposition reaction and the crystalline quality of the Si islands.

Scanning electron microscopy, in conjunction with electron channeling, showed that the Si remaining in the island region was single crystalline with approximately the same orientation as the substrate Si. The W reaction begins between the islands, where the overlayer Si was removed down to the buried porous Si layer, and proceeds from the edge toward the center of the islands. The extent of the W deposition was easily seen by tilting the

sample in the SEM to 70° in order to obtain a cross-sectional view. Figure 2 shows a backscattered electron image of the sample in cross section. The buried W was deposited under the island leaving a small gap of porous Si centered below the island.

NMA (with both RBS and HIXE) was done to determine the extent of a silicide-forming reaction between the Si in the islands and the deposited W. The RBS data was collected by scanning an 8.7 MeV He beam (3 μm in diameter) in a line 100 μm long across the Si islands. The yield of backscattered ions versus energy was collected at each point along the scan and several spectra from each point were summed to improve statistics. The concentration versus depth, determined from the RBS spectra for 4 regions of the sample, are plotted in figure 2. These results indicate that the W reacts with the sides of the Si islands forming a silicide. This silicide region is uniform and approximately 3 μm thick on both sides of the island. Further, the discontinuity in the buried W layer was found to be a 3 μm wide region of unreacted porous Si beneath the center of the Si island. A study of the W deposition and silicide formation kinetics is planned by repeating the NMA measurements for various times during the LPCVD process.

A comparison of the resolution limits for NMA and SEM-based composition analysis shows that the nuclear microprobe yields both unique and complementary quantitative composition information. Current nuclear microprobes have a lateral resolution which is a factor of 10 poorer than the lateral resolution in an SEM; but, SEM analyses have very limited depth resolution, whereas NMA has a depth resolution down to 10 nm for 2 MeV ion scattering. The lack of depth resolution in the SEM is a particular problem when analyzing layered samples in which the x-ray peaks of elements from different layers overlap (e.g., thin-film superconductors on $SrTiO_3$

substrates). The NMA yields a three-dimensional analysis of the composition in which the effects of the substrate can be easily separated from that of the thin film. Further, the nuclear microprobe is compatible with several techniques such as RBS, EBS, and ERD, which not only give compositional information on heavy elements (from the third row of the periodic table and above) but also give quantitative analyses on elements in the first two rows of the periodic table.

REFERENCES

1. B. L. Doyle et al., Microbeam Analysis--1981, 79-86.

2. B. L. Doyle, Microbeam Analysis--1986, 15-21.

3. B. L. Doyle, 12th International Symposium on Applications of Ion-Beams in Materials Science--Hosei University Press, Tokyo, 153 (1988).

4. R. Beyers, G. Lim, E. M. Engler, V. Y. Lee, M. L. Ramirez, R. J. Savoy, R. D. Jacowitz, T. M. Shaw, S. La Placa, R. Boehme, C. C. Tsuei, Sung I. Park, M. W. Shafer, and W. J. Gallagher, Appl. Phys. Lett. 51, 614 (1987).

5. H. U. Krebs and R. Wordenweber, J. Appl. Phys. 63, 1642 (1988).

6. J. A. Knapp, private communication.

7. W-K. Chu, J. W. Mayer, and M-A. Nicolet, Backscattering Spectrometry, (Academic Press, New York, 1978), pp. 21-218.

8. J. C. Barbour, B. L. Doyle, and S. M. Myers, Phys. Rev. B 38, 7005 (1988).

9. R. S. Blewer, S. S. Tsao, and G. M. Gutierrez, Mat. Res. Soc. Symp. Proc. 107, 287 (1988).

FIGURE CAPTIONS

FIG. 1.-- Both RBS and HIXE were used to obtain elemental maps of the Y-Ba-Cu-O alloy. The gray scale for the HIXE maps is such that a dark region represents a high intensity of x-rays. The RBS spectra were collected using

a 2 μm diameter beam from the two regions (dark and light) indicated by the arrows in the Y-HIXE map.

FIG. 2.-- Backscattered electron image of the edge of a silicon wafer which was treated to form buried W layers beneath epitaxial (epi) Si islands. The sample was tilted 70° to obtain the SEM image. The four depth scales shown at right were measured from RBS spectra collected in a line scan accross the Si islands. The concentration of W is given in atoms/cm^3. Note: the zero for the depth scale in A begins at the W surface which is 3 μm deeper than the surface of the Si island. The Si profiles are shown only as a reference for the relative position of the W and Si signals in the RBS spectra. The oscillatory Si concentration as a function of depth results from the non-Rutherford Si cross section which was not deconvoluted from these profiles.

Y-Ba-Cu-O ALLOY, MIXED PHASES, 123 AND 211

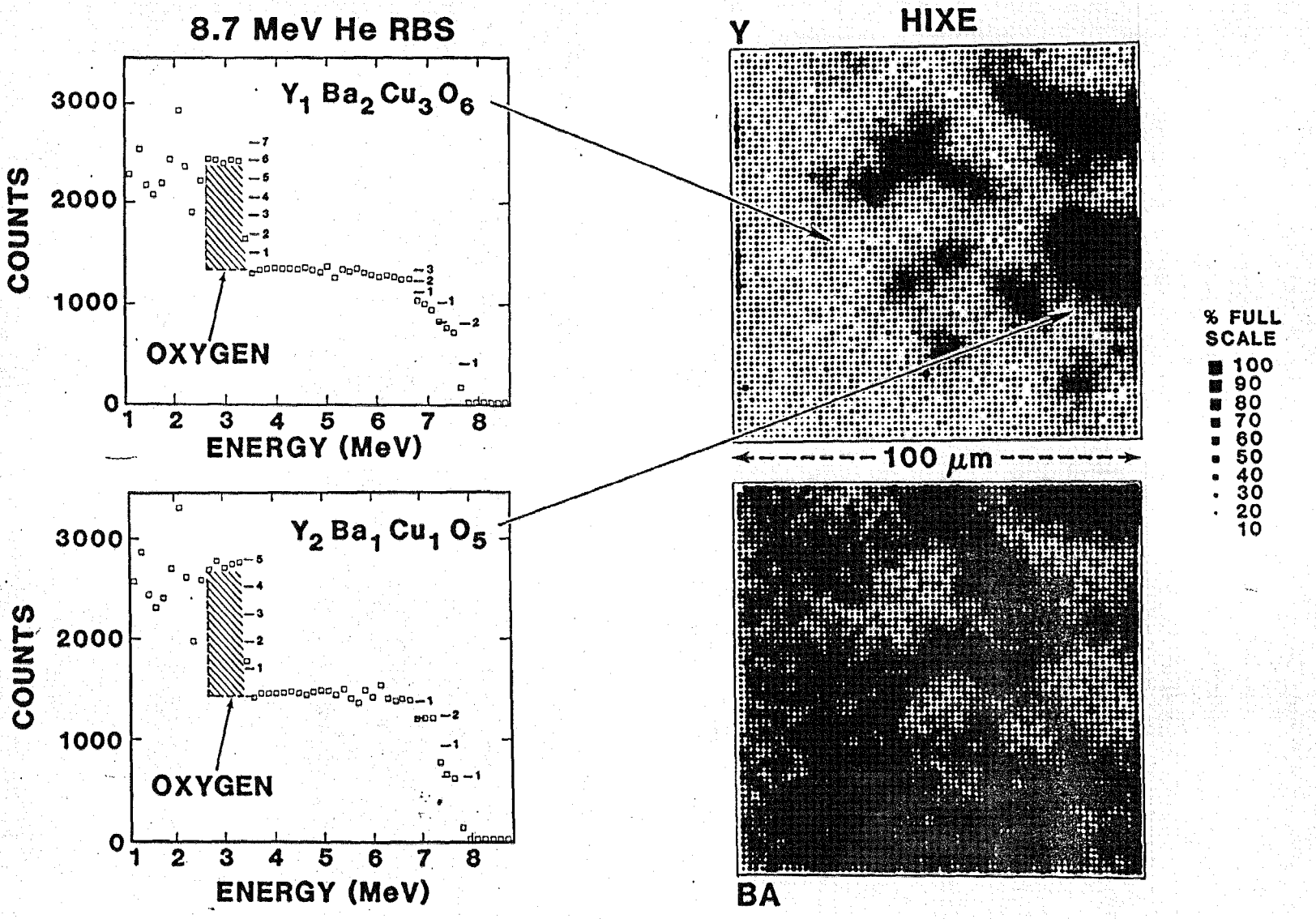

8.7 MeV He^{++}
BACKSCATTERING

3 μm PROBE

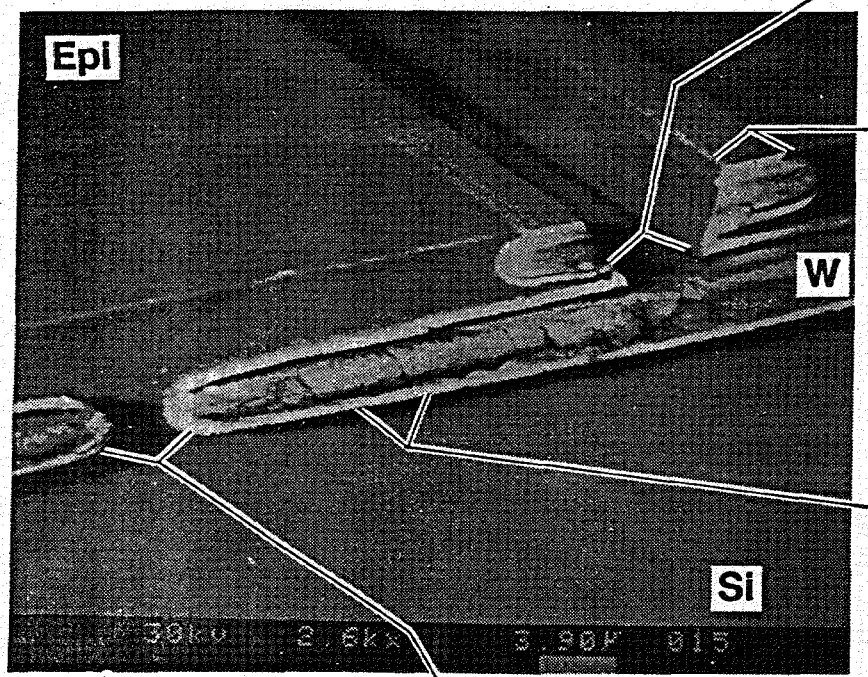

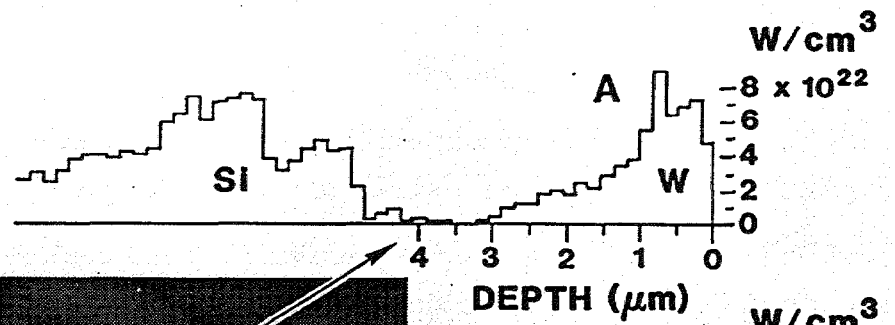

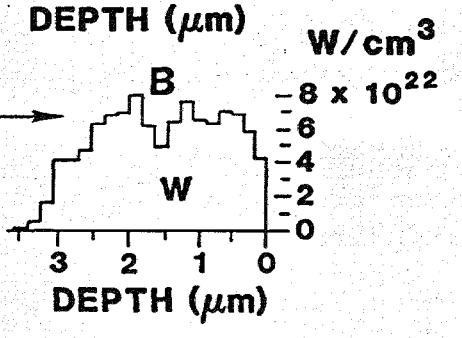

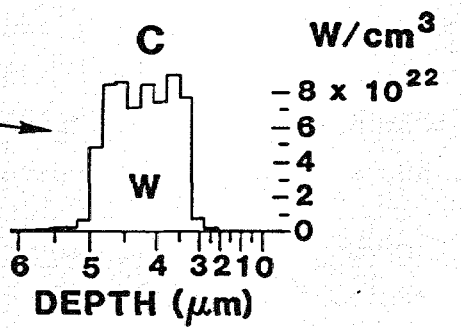

BURIED W LAYER
IN (100) Si